



TITLE:

Dielectric Analysis of Interfacial Polarization in Bilamellar Structure as Applied to Underwater Polystyrene Films

AUTHOR(S):

Zhang, Hezhe; Hanai, Tetsuya; Koizumi, Naokazu

CITATION:

Zhang, Hezhe ...[et al]. Dielectric Analysis of Interfacial Polarization in Bilamellar Structure as Applied to Underwater Polystyrene Films. Bulletin of the Institute for Chemical Research, Kyoto University 1983, 61(4): 265-281

ISSUE DATE:

1983-11-25

URL:

<http://hdl.handle.net/2433/77046>

RIGHT:

Dielectric Analysis of Interfacial Polarization in Bilamellar Structure as Applied to Underwater Polystyrene Films

Hezhe ZHANG*, Tetsuya HANAI**, and Naokazu KOIZUMI**

Received July 2, 1983

With a view to evaluating relative permittivity and electrical conductivity of underwater polystyrene films, theoretical formulas of interfacial polarization for bilamellar structure were applied to dielectric observations for systems consisting of the film and the aqueous solution. General formulas of the theory were derived to calculate capacitances and conductances of the film and the aqueous phase from the dielectric relaxation shown by the film-aqueous solution systems. Approximate formulas were derived from the general formulas under the condition that the observed capacitance at low frequencies is much higher than that at high frequencies. Examination of the formulas in dielectric observations for the lumped impedance models showed that the general formulas gave the capacitances and conductances of the constituents within errors of 1.5%, whereas the approximate formulas can be used in practice under a limited condition. The general formulas were further applied to the dielectric observations on systems of underwater polystyrene films to obtain the film capacitance and conductance. The results showed that the film capacitance was unaffected by the electrolyte species and the concentrations of the ambient aqueous solutions, giving the film permittivity of 2.65.

KEY WORDS: Dielectric relaxation/ Electrical conductivity/ Interfacial polarization/ Maxwell-Wanger relaxation/ Permittivity/ Polystyrene film/

I. INTRODUCTION

In a previous study,¹⁾ an attempt was made to estimate relative permittivity and electrical conductivity of underwater polystyrene films from dielectric observations on a series combination of the film and the ambient aqueous solution. The approximate formulas used in the analysis of the observations were derived from a dielectric theory of interfacial polarization for the bilamellar structure under the two conditions that the film capacitance is much higher than that of the aqueous solutions, and that the film conductance is lower than that of the aqueous solutions. This is not necessarily the case with a variety of combinations of the films and the electrolyte solutions. It is desirable that the capacitance and the conductance of the underwater films should be evaluated without such restrictions.

In the present paper, general formulas are proposed to calculate capacitances and conductances of the constituent phases from dielectric observations on the interfacial

* 張 河哲: Department of Chemistry, Northeast Normal University, Changchun, China.

** 花井哲也, 小泉直一: Laboratory of Dielectrics, Institute for Chemical Research, Kyoto University, Uji, Kyoto 611, Japan.

polarization due to bilamellar structure. Approximate formulas are also derived from those of the general procedure under the conditions mentioned above. Both the general and the approximate formulas are applied to dielectric observations for some model systems composed of solid capacitors and resistors to discuss the validity of these formulas. Application of the formulas is made further to systems of polystyrene films immersed in electrolyte solutions to obtain the capacitance and the conductance of the underwater films.

II. THEORETICAL FORMULAS TO CALCULATE PHASE PARAMETERS FROM DIELECTRIC PARAMETERS OBSERVED

2.1 General Formulas of Dielectric Parameters for Bilamellar Structure

Composite dielectrics in bilamellar structure can be simulated with a series combination of Phase *a* (the capacitance C_a , and the conductance G_a) and phase *b* (C_b , G_b) as illustrated in Fig. 1A, which can be measured with an ac bridge in terms of the parallel-equivalent capacitance C and the parallel-equivalent conductance G as shown in Fig. 1B.

According to impedance calculation, the limiting values of C and G at high frequencies (subscript *h*) and at low frequencies (subscript *l*) and the relaxation frequency f_0 are given by the following relations:²⁾

$$C_h = \frac{C_a C_b}{C_a + C_b}, \quad (1a)$$

$$G_h = \frac{G_a C_b^2 + G_b C_a^2}{(C_a + C_b)^2}, \quad (2)$$

$$G_l = \frac{G_a G_b}{G_a + G_b}, \quad (3a)$$

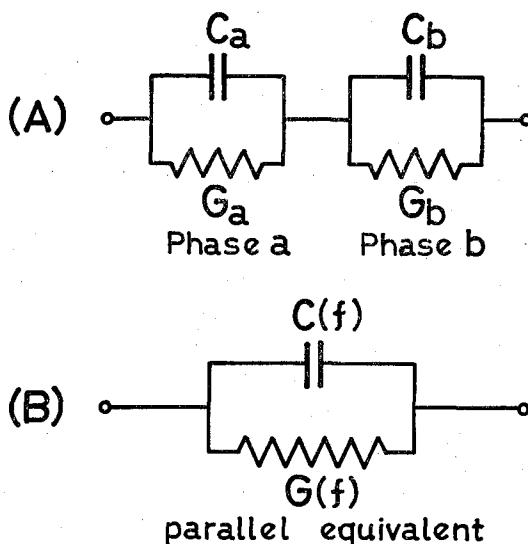


Fig. 1. (A) Lumped impedance model for bilamellar structure consisting of Phase *a* (the capacitance C_a and the conductance G_a) and Phase *b* (C_b , G_b), and (B) its equivalent model composed of the parallel-equivalent capacitance C and the parallel-equivalent conductance G .

$$C_l = \frac{C_a G_b^2 + C_b G_a^2}{(G_a + G_b)^2}, \quad (4)$$

and

$$f_0 = \frac{1}{2\pi} \cdot \frac{G_a + G_b}{C_a + C_b}. \quad (5)$$

If Y_a and Y_b are defined respectively by

$$Y_a \equiv \frac{C_b}{C_a}, \quad \text{and} \quad Y_b \equiv \frac{C_a}{C_b}, \quad (1b)$$

then Eq. 1a is transformed to

$$\frac{1}{C_b} = \frac{1}{C_a} (1 - Y_a), \quad (1c)$$

and

$$\frac{C_a}{C_b} = \frac{1}{Y_a} - 1. \quad (1d)$$

If X_a and X_b are defined respectively by

$$X_a \equiv \frac{G_l}{G_a}, \quad \text{and} \quad X_b \equiv \frac{G_l}{G_b}, \quad (3b)$$

then Eq. 3a is transformed to

$$\frac{1}{G_b} = \frac{1}{G_l} (1 - X_a), \quad (3c)$$

and

$$\frac{G_a}{G_b} = \frac{1}{X_a} - 1. \quad (3d)$$

By use of Eqs. 1a and 3a, Eqs. 1b and 3b are reduced to the following, respectively:

$$Y_a + Y_b = 1, \quad (6)$$

and

$$X_a + X_b = 1. \quad (7)$$

2.2 Inequalities Concerning Relative Magnitude between G_a/C_a and G_b/C_b

For the convenience of further consideration, a quantity B is defined by

$$B \equiv \frac{G_b}{C_b} - \frac{G_a}{C_a}. \quad (8)$$

By use of Eqs. 1a, 2, 3a, and 4, we have

$$\frac{C_a}{G_a} - \frac{C_l}{G_l} = \frac{C_a C_b}{G_b (G_a + G_b)} B, \quad (9)$$

$$\frac{G_b}{C_b} - \frac{G_b}{C_a} = \frac{C_b}{C_a + C_b} B, \quad (10)$$

$$\frac{C_l}{G_l} - \frac{C_b}{G_b} = \frac{C_a C_b}{G_a(G_a + G_b)} B, \quad (11)$$

and

$$\frac{G_h}{C_h} - \frac{G_a}{C_a} = \frac{C_a}{C_a + C_b} B. \quad (12)$$

Since the sign of left sides of Eqs. 9 to 12 is the same as the sign of B , the following inequalities are readily derived:

$$\frac{G_a}{C_a} < \frac{G_l}{C_l} < \frac{G_l}{C_h} < \frac{G_h}{C_h} < \frac{G_b}{C_b} \quad \text{for } B > 0, \quad (13)$$

and

$$\frac{G_b}{C_b} < \frac{G_l}{C_l} < \frac{G_l}{C_h} < \frac{G_h}{C_h} < \frac{G_a}{C_a} \quad \text{for } B < 0. \quad (14)$$

The inequalities Eqs. 13 and 14 can be depicted comprehensibly by means of C-G plane representation as shown in Fig. 2. A point \bar{C} on the C-G plane is specified with a number-pair (C, G) , of which the first number C denotes the abscissa and the second number G means the ordinate of the plane. On the C-G planes shown in Fig. 2, some points relevant to Eqs. 13 and 14 are specified with the following parenthesized number-pairs:

$$\begin{aligned} \bar{C}_a &= (C_a, G_a), \quad \bar{C}_l = (C_l, G_l), \quad \bar{C}_{hl} = (C_h, G_l), \\ \bar{C}_b &= (C_b, G_b), \quad \bar{C}_h = (C_h, G_h), \quad \bar{C}_{lh} = (C_l, G_h). \end{aligned} \quad (15)$$

With change in frequency, the capacitance C and the conductance G defined with Fig. 1B vary along a straight line locus $\bar{C}_l \bar{C}_h$ on the C-G planes shown in Fig. 2.

According to Eq. 13, the arguments (amplitude) of the vectors \bar{C} 's in Fig. 2A for

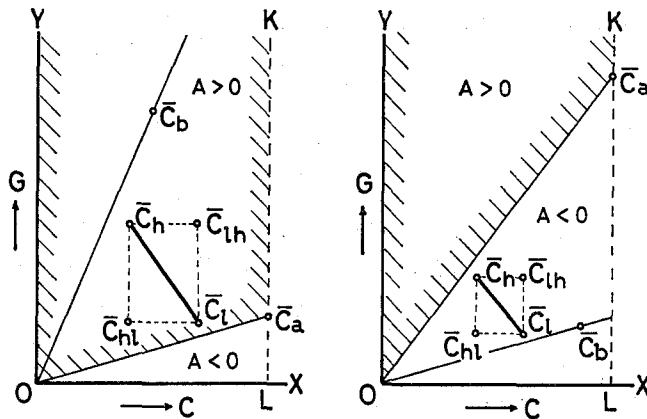


Fig. 2A The case with $B > 0$

Fig. 2B The case with $B < 0$

Fig. 2. Location of Points \bar{C}_l (with C_l and G_l), \bar{C}_h (C_h , G_h), \bar{C}_{hl} (C_h , G_l) and \bar{C}_{lh} (C_l , G_h) relative to Points \bar{C}_a (C_a , G_a) and \bar{C}_b (C_b , G_b) on the capacitance C (abscissa) versus conductance G (ordinate) plane under the condition $C_a > C_b$. The hatched areas denote the domains with $A > 0$.

$B > 0$ are aligned in the following order:

$$\bar{C}_a < \bar{C}_l < \bar{C}_{hl} < \bar{C}_h < \bar{C}_b.$$

Similarly Eq. 14 explains the alignment of the arguments of the vectors \bar{C} 's as shown in Fig. 2B for $B < 0$.

2.3 Derivation of General Formulas of Phase Parameters

In principle, the present problem is to solve four simultaneous equations 1a, 2, 3a, and 4 so as to have explicit function forms with respect to four variables C_a , C_b , G_a and G_b .

Substituting Eqs. 1d, 3c and 3d for Eq. 2, we have

$$G_h = \frac{\frac{G_a}{G_b} + \left(\frac{C_a}{C_b}\right)^2}{\frac{1}{G_b} \left(\frac{C_a}{C_b} + 1\right)^2} = \frac{\left(\frac{1}{X_a} - 1\right) + \left(\frac{1}{Y_a} - 1\right)^2}{\frac{1}{G_l} (1 - X_a) \left(\frac{1}{Y_a}\right)^2}. \quad (16)$$

The rearrangement of Eq. 16 gives

$$(Y_a - X_a)^2 = X_a(1 - X_a) \left(\frac{G_h}{G_l} - 1\right). \quad (17)$$

By the aid of Eqs. 13 and 14, Eq. 17 is solved for Y_a as

$$Y_a = X_a \begin{cases} - \\ + \end{cases} \left\{ X_a(1 - X_a) \left(\frac{G_h}{G_l} - 1\right) \right\}^{1/2} \quad \text{for} \quad \begin{cases} Y_a < X_a, B > 0. \\ Y_a > X_a, B < 0. \end{cases} \quad (18)$$

$$(19)$$

In a similar manner, substitution of Eqs. 1c, 1d, and 3d for Eq. 4 gives

$$C_l = \frac{\frac{C_a}{C_b} + \left(\frac{G_a}{G_b}\right)^2}{\frac{1}{C_b} \left(\frac{G_a}{G_b} + 1\right)^2} = \frac{\left(\frac{1}{Y_a} - 1\right) + \left(\frac{1}{X_a} - 1\right)^2}{\frac{1}{C_h} (1 - Y_a) \left(\frac{1}{X_a}\right)^2}. \quad (20)$$

The rearrangement of Eq. 20 gives

$$(Y_a - X_a)^2 = Y_a(1 - Y_a) \left(\frac{C_l}{C_h} - 1\right). \quad (21)$$

By the aid of Eqs. 13 and 14, Eq. 21 is solved for X_a as

$$X_a = Y_a \begin{cases} + \\ - \end{cases} \left\{ Y_a(1 - Y_a) \left(\frac{C_l}{C_h} - 1\right) \right\}^{1/2} \quad \text{for} \quad \begin{cases} Y_a < X_a, B > 0. \\ Y_a > X_a, B < 0. \end{cases} \quad (22)$$

$$(23)$$

Equating Eq. 17 to Eq. 21, and eliminating X_a by use of either Eq. 22 or Eq. 23, we have, after tedious calculations,

$$\frac{1 - 2Y_a}{\{Y_a(1 - Y_a)\}^{1/2}} = \begin{cases} + \\ - \end{cases} A \quad \text{for} \quad \begin{cases} B > 0, \\ B < 0, \end{cases} \quad (24)$$

$$(25)$$

where

$$A \equiv \left\{ \left(1 - \frac{G_l}{G_h} \right)^{-1} - \left(\frac{C_l}{C_h} - 1 \right)^{-1} \right\} \left(\frac{C_l}{C_h} - 1 \right)^{1/2}. \quad (26)$$

Both Eq. 24 and Eq. 25 squared give

$$Y_a^2 - Y_a + \frac{1}{4+A^2} = 0, \quad \text{for both } B > 0 \text{ and } B < 0. \quad (27)$$

As regards the lumped impedance circuit shown in Fig. 1A, the same values of dielectric parameters C_l , C_h , G_l and G_h are observed even if Phase a and b are interchanged. Therefore, two roots of the quadratic Eq. 27 are to give Y_a and Y_b . In the succeeding calculations, smaller one of the two roots of Eq. 27 is assumed to be Y_a and larger one to be Y_b without loss in generality, leading to a relation

$$C_a > C_b. \quad (28)$$

Hence Eq. 27 is solved to give the two roots, which are designated Y_a and Y_b respectively as

$$Y_a = \frac{1}{2} - \frac{1}{2} \left\{ 1 + \left(\frac{2}{A} \right)^2 \right\}^{-1/2} \leq \frac{1}{2}, \quad (29)$$

and

$$Y_b = \frac{1}{2} + \frac{1}{2} \left\{ 1 + \left(\frac{2}{A} \right)^2 \right\}^{-1/2} \geq \frac{1}{2}. \quad (30)$$

By use of Eqs. 1b and 6, C_a and C_b are given by

$$C_a = \frac{C_h}{Y_a}, \quad (31)$$

and

$$C_b = \frac{C_h}{Y_b} = \frac{C_h}{1 - Y_a}. \quad (32)$$

Since Y_a represented by Eq. 29 gives the following inequality

$$1 - 2Y_a \geq 0, \quad (33)$$

Eqs. 24 and 25 give the features that

$$\text{if } A > 0, \text{ then } B > 0, \quad \text{referring to Fig. 2A,} \quad (34)$$

and

$$\text{if } A < 0, \text{ then } B < 0, \quad \text{referring to Fig. 2B.} \quad (35)$$

Hence Eqs. 22 and 23 result in the following relations:

$$X_a = Y_a + \left\{ Y_a(1 - Y_a) \left(\frac{C_l}{C_h} - 1 \right)^{1/2} \right\} \quad \text{for } A > 0, \quad (36)$$

and

$$X_a = Y_a - \left\{ Y_a(1 - Y_a) \left(\frac{C_l}{C_h} - 1 \right)^{1/2} \right\} \quad \text{for } A < 0, \quad (37)$$

For both Eqs. 36 and 37, we have

$$G_a = \frac{G_l}{X_a} \quad (38)$$

and

$$G_b = \frac{G_l}{X_b} = \frac{G_l}{1 - X_a} \quad (39)$$

Substitution of Eqs. 31, 32, 38 and 39 for Eq. 5 gives

$$f_0 = \frac{1}{2\pi} \cdot \frac{G_h - G_l}{C_l - C_h} \quad (40)$$

The general procedure to calculate the phase parameters is summarized as follows:

Dielectric parameters C_l , C_h , G_l , G_h observed are substituted into Eq. 26 to calculate the value of A . Values of C_a and C_b are calculated by use of Eqs. 29, 30, 31 and 32. In this instance, the value of C_a is for larger one of the two lumped capacitances. The value of Y_a obtained is substituted into Eq. 36 when $A > 0$, and into Eq. 37 when $A < 0$ to calculate X_a , which is substituted into Eqs. 38 and 39 to calculate G_a and G_b . The relaxation frequency f_0 is calculated from C_l , C_h , G_l and G_h by use of Eq. 40.

2.4 Representation of the Quantity A by Use of Phase Parameters

The quantity A given by Eq. 26 is represented by phase parameters C_a and C_b as shown below.

By use of Eqs. 1a and 4, we have

$$\frac{C_l}{C_h} - 1 = \frac{C_a C_b B^2}{(G_a + G_b)^2} \quad (41)$$

Using Eqs. 2 and 3a, we have

$$1 - \frac{G_l}{G_h} = \frac{C_a^2 C_b^2 B^2}{(G_a + G_b)(G_a C_b^2 + G_b C_a^2)} \quad (42)$$

Substitution of Eqs. 41 and 42 for Eq. 26 gives

$$A = \frac{(B^2)^{1/2}}{B} \cdot \frac{C_a - C_b}{(C_a C_b)^{1/2}} = \begin{cases} + \frac{C_a - C_b}{(C_a C_b)^{1/2}} & \text{for } B > 0. \\ - \frac{C_a - C_b}{(C_a C_b)^{1/2}} & \text{for } B < 0. \end{cases} \quad (43)$$

The sign of A given by Eqs. 43 and 44 is associated with the inter-location between \bar{C}_a and \bar{C}_b on the C - G plane. According to Eq. 43, the relation $A > 0$ holds when the point \bar{C}_b is located in a domain $K\bar{C}_aOY$ above a line \bar{C}_aO as seen in Fig. 2A. Equation 44 means that the relation $A < 0$ holds when the point \bar{C}_b is located in a domain \bar{C}_aOL below the line \bar{C}_aO as shown in Fig. 2B. The sign of A is, therefore, predictable provided that the location of \bar{C}_b relative to the line \bar{C}_aO is appointed.

When the point \bar{C}_b is located just on the line \bar{C}_aO , the function A given by Eqs. 43 and 44 is discontinuous with respect to the change in B , and is a double-valued function. In this instance, the dielectric relaxation vanishes owing to $B = 0$.

2.5 Derivation of Approximate Formulas

In the previous paper,¹⁾ approximate formulas were derived for C_a , C_b , G_a and G_b in the bilamellar structure as shown in Fig. 1 under two conditions:

$$C_a \gg C_b, \quad \text{and} \quad G_a \lesssim G_b. \quad (45)$$

As a matter of fact, it is impracticable to confirm these conditions prior to the evaluation of such phase parameters C_a and C_b .

In the present paper, we adopt a condition represented by dielectric parameters C_l and C_h which can be known from observations as follows:

$$C_l \gg C_h. \quad (46)$$

This condition Eq. 46 is rearranged to

$$\frac{C_l}{C_h} \gg 1, \quad \text{and} \quad \frac{C_h}{C_l} \ll 1. \quad (47)$$

By use of Eq. 47, Eq. 26 is transformed to

$$\begin{aligned} A &\approx \left(\frac{G_h}{G_h - G_l} - \frac{C_h}{C_l} \right) \left(\frac{C_l}{C_h} \right)^{1/2}, \\ &\approx \frac{G_h}{G_h - G_l} \left(\frac{C_l}{C_h} \right)^{1/2} > 1 > 0. \end{aligned} \quad (48)$$

The square of Eq. 48 gives

$$A^2 = \left(\frac{G_h}{G_h - G_l} \right)^2 \frac{C_l}{C_h} \gg 1. \quad (49)$$

and

$$\left(\frac{2}{A} \right)^2 = \frac{4}{A^2} \ll 1. \quad (50)$$

By the method of expansion in the Taylor series, Eqs. 29 and 30 approximate to

$$\frac{Y_a}{Y_b} \approx \frac{1}{2} - \frac{1}{2} \left\{ 1 - \frac{1}{2} \left(\frac{2}{A} \right)^2 \right\}. \quad (51)$$

Thus we have

$$Y_a = \frac{1}{A^2} \ll 1, \quad (52)$$

and

$$Y_b = 1 - \frac{1}{A^2} \approx 1. \quad (53)$$

As regards the expressions of X_a , Eq. 36 is adopted in consideration of Eq. 48. Substitution of Eqs. 47, 52, 48 and 49 for Eq. 36 gives

$$X_a = \frac{G_h - G_l}{G_h}. \quad (54)$$

Equation 54 is substituted for Eq. 7, giving

$$X_b = 1 - X_a = \frac{G_l}{G_h}. \quad (55)$$

Equation 31, 32, 38, 39 and 40 are rewritten as

$$C_a = \frac{C_h}{Y_a} = C_l \left(\frac{G_h}{G_h - G_l} \right)^2, \quad (56)$$

$$C_b = \frac{C_h}{Y_b} = C_h, \quad (57)$$

$$G_a = \frac{G_l}{X_a} = G_l \frac{G_h}{G_h - G_l}, \quad (58)$$

$$G_b = \frac{G_l}{X_b} = G_h, \quad (59)$$

and

$$f_0 = \frac{1}{2\pi} \cdot \frac{G_h - G_l}{C_l}. \quad (60)$$

Equations 56 to 60 are the same as those derived in the previous paper¹⁾ under the conditions Eq. 45. Hence Eq. 46 seems to be equivalent to Eq. 45.

2.6 Formulas for Relative Permittivity and Conductivity

Provided that the values of C_a , G_a , G_b and C_b are known from Eqs. 31, 32, 38 and 39 for the general formulas and from Eqs. 56 to 59 for the approximate formulas, the relative permittivity ϵ_a and the electrical conductivities κ_a and κ_b of each phase are calculated by use of the following relations:

$$\epsilon_a = C_a \frac{t}{S \epsilon_v}, \quad (61)$$

$$\kappa_a = G_a \frac{t}{S}, \quad (62)$$

$$\kappa_b = G_b \frac{l}{A} = G_b \frac{\epsilon_b \epsilon_v}{C_b}, \quad (63)$$

where t and S are the thickness and the area of Phase a , and l and A are the thickness and the area of Phase b respectively.

When the value of l cannot be accurately determined, the relative permittivity ϵ_b and the permittivity of vacuum $\epsilon_v = 8.8542 \times 10^{-14} \text{ F cm}^{-1}$ are adopted for evaluating κ_b from Eq. 63.

III. EXAMINATION IN APPLICABILITY OF THE FORMULAS BY USE OF LUMPED IMPEDANCE MODELS

The formulas derived above were applied to dielectric observations for lumped impedance Models A, B, C, and D consisting of capacitors (the capacitances C_a and C_b) and resistors (the conductances G_a and G_b), the values of which are listed in Table I.

Table I. Dielectric Parameters Observed and Phase Parameters Calculated for Lumped Impedance Models Consisting of Solid Capacitors and Solid Resistors

	Phase parameters					$A^{e)}$	Dielectric parameters observed							$A^{g)}$
	$\frac{C_a}{\text{pF}}$	$\frac{C_b}{\text{pF}}$	$\frac{G_a}{\mu\text{S}}$	$\frac{G_b}{\mu\text{S}}$	$\frac{f_0}{\text{kHz}}$		$\frac{C_l}{\text{pF}}$	$\frac{C_h}{\text{pF}}$	$\frac{G_l}{\mu\text{S}}$	$\frac{G_h}{\mu\text{S}}$	$\frac{C_l}{C_h}$	$\frac{f_0^{(d)}}{\text{kHz}}$		
Model A														
Observed ^{a)}	381.6	221.7	4.998	1.020	1.59 ^{d)}	-0.5497	165	139.6	0.840	1.099	1.182	1.56	-0.5344	
Calc. by														
general ^{b)}	376.4	221.9	5.095	1.006	1.62									
approx. ^{c)}	2971.	139.6	3.564	1.099	0.25									
Model B														
Observed ^{a)}	381.6	99.38	1.020	4.998	1.99 ^{d)}	1.449	264.7	78.7	0.840	3.208	3.363	2.0	1.432	
Calc. by														
general ^{b)}	376.7	99.48	1.007	5.056	2.03									
approx. ^{c)}	485.8	78.7	1.138	3.208	1.42									
Model C														
Observed ^{a)}	972.5	99.38	1.020	4.998	0.894 ^{d)}	2.808	675.9	90.29	0.840	4.12	7.485	0.90	2.806	
Calc. by														
general ^{b)}	972.7	99.53	1.010	4.996	0.891									
approx. ^{c)}	1066	90.29	1.055	4.12	0.772									
Model D														
Observed ^{a)}	2001	19.83	1.020	4.998	0.474 ^{d)}	9.947	1388.	19.75	0.842	4.89	70.28	0.480	9.934	
Calc. by														
general ^{b)}	2008	19.94	1.013	4.988	0.471									
approx. ^{c)}	2025	19.75	1.017	4.89	0.464									

a) Observed directly for each capacitor and resistor.

b) Calculated from the observed C_l , C_h , G_l and G_h by use of the general formulas Eqs. 26 and 29 to 40.

c) Calculated from the observed C_l , C_h , G_l and G_h by use of the approximate formulas Eqs. 56 to 60.

d) Calculated from the directly observed C_a , C_b , G_a and G_b by use of Eq. 5.

e) Calculated from the directly observed C_a and C_b by use of Eq. 43 or Eq. 44.

f) Obtained by interpolation from the dielectric relaxations observed.

g) Calculated from the observed C_l , C_h , G_l and G_h by use of Eq. 26.

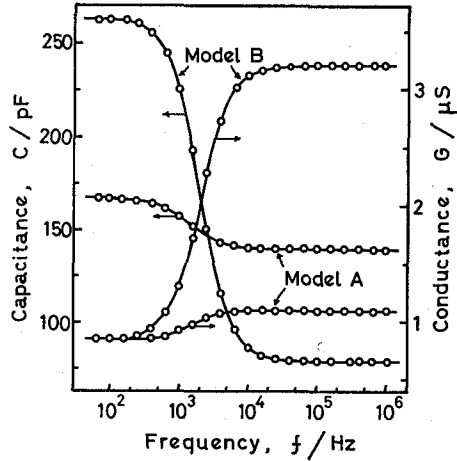


Fig. 3A. Frequency dependence of the parallel-equivalent capacitance C and the parallel-equivalent conductance G for lumped impedance Models A and B.

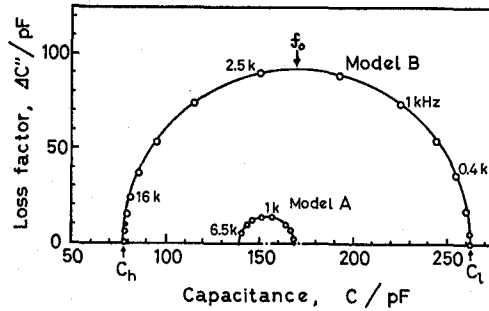


Fig. 3B. Complex plane plots of the complex capacitance $C^* = C - j\Delta C''$ for lumped impedance Models A and B. The same data as shown in Fig. 3A. Loss factor, $\Delta C'' = (G - G_l)/(2\pi f)$.

First of all, each value of C_a , C_b , G_a , and G_b was measured directly. Next, these four elements were combined with one another as shown in Fig. 1A, the parallel-equivalent capacitance C and conductance G having been measured over the frequency range shown below. These Models showed marked dielectric relaxations as shown in Figs. 3A and 3B, in which the values of C_l , C_h , G_l , G_h , and f_0 were obtained with accuracy.

From these values of C_l , C_h , G_l , and G_h , phase parameters C_a , C_b , G_a , G_b and f_0 were calculated by use of the general formulas Eqs. 26 to 40 and of the approximate formulas Eqs. 56 to 60, being listed in Table I.

For Models A, B, C and D, the values of C_a , C_b , G_a and G_b calculated by use of the general formulas are in agreement with the directly observed values within errors less than 1.5%, which are not caused by the defect of the general formulas but are attributed mainly to the errors of observation.

The results by use of the approximate formulas were seriously affected by the

values of C_i/C_h . For Model A ($C_i/C_h \approx 1$), the approximate formulas give very erroneous values for C_a , C_b , G_a and G_b . The error of C_a by use of the approximate formula Eq. 56 amounts to as much as 680%. For Model B ($C_i/C_h \approx 3$) and Model C ($C_i/C_h \approx 7$), the errors of C_a are 27 and 10% respectively. For Model D ($C_i/C_h \approx 70$), the errors of C_a is only 1%. It is concluded, therefore, that the approximate formulas Eqs. 56 to 60 may be put to use when $C_i/C_h \gtrsim 70$.

IV. APPLICATION TO UNDERWATER POLYSTYRENE FILMS

4.1 Experimental Setup

The preparation of cast polystyrene films was the same as described before.¹⁾ Polystyrene-dichloromethane (1%, w/v) solutions were spread on a glass plate, and were allowed to stand to be dried up. Thin films cast on the glass plate were mounted on a measuring cell, which is shown in Fig. 4. Both the compartments of the measuring cell were filled with the same aqueous solution of some electrolytes which are shown below.

The parallel-equivalent capacitance C and the parallel-equivalent conductance G of the measuring cell systems were measured with a TR-1C Transformer Ratio-Arm Bridge of Ando Electric Co. Ltd. over the frequency range 20 Hz to 3 MHz at 20°C.

4.2 Application of the Formulas to the Underwater Polystyrene Films

Figure 5 shows frequency dependence of the capacitance C and the conductance G observed for the cell system with a polystyrene film and the compartments which were filled with NaOH solutions in different concentrations. Complex plane plots of the complex capacitance for the same data are shown in Fig. 6, which gave semicircles demonstrating the lumped impedance model shown in Fig. 1A.

Values of C_i , C_h , G_i , G_h and the relaxation frequency f_0 can readily be obtained from Figs. 5 and 6, being used for calculating values of C_a , C_b , G_a , G_b , and f_0 by use of the general formulas Eq. 26 to Eq. 40 and of the approximate formulas Eq. 56 to Eq. 60.

In a similar manner, dielectric observations and the succeeding data processing

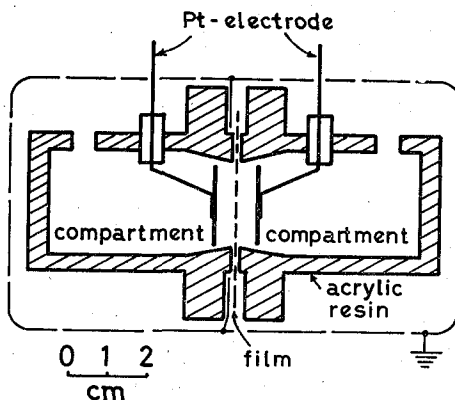


Fig. 4. A cell system for measuring dielectric properties of thin films immersed in aqueous solutions.

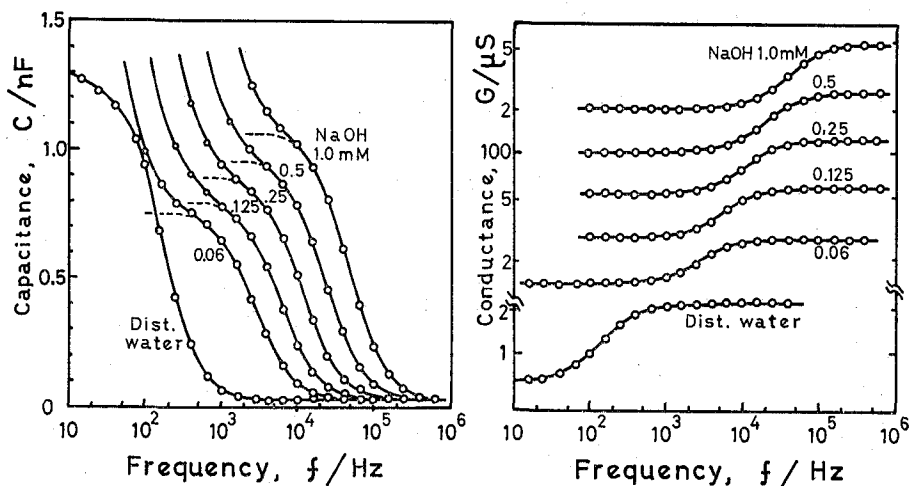


Fig. 5. Frequency dependence of the parallel-equivalent capacitance C and the parallel-equivalent conductance G for the cell systems with a polystyrene film and the ambient NaOH solutions in 1, 0.5, 0.25, 0.125, 0.06 and 0 mM.

were repeated for the cell systems with the same film and the ambient aqueous solutions with KOH and polystyrene sulfonate. Table II lists the values of dielectric parameters C_l , C_h , G_l , G_h and f_0 observed and those of phase parameters C_a , C_b , G_a , G_b and f_0 calculated.

Since the values of C_l/C_h observed are ranging from 25 to 52, the results derived with the approximate formulas include errors amounting to 5%, and are not always usable for quantitative consideration. The following discussion, therefore, will be made only on the results by the general formulas.

It was reported in references³⁻⁶⁾ that polystyrene sulfonate solutions show dielectric relaxations in a kHz-region. Also in the present study, another minute dielectric relaxation was observed for the film-solution systems as well as for the solutions only

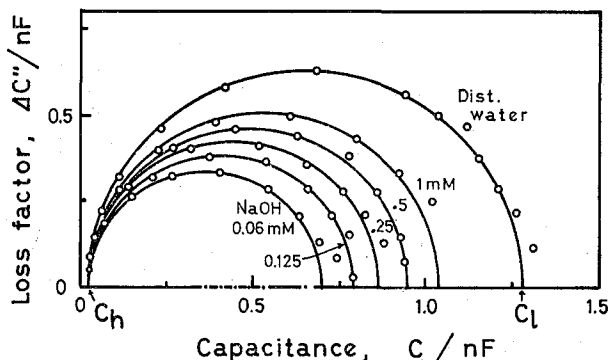


Fig. 6. Complex plane plots of the complex capacitance $C^* = C - j\Delta C''$ for the cell systems with polystyrene film and the ambient NaOH solutions in 1, 0.5, 0.25, 0.125, 0.06 and 0 mM. The data referring to Fig. 5.

Table II. Dielectric Parameters Observed and Phase Parameters Calculated for the Cell Systems with a Polystyrene Film and the Ambient Electrolyte Solutions at 20°C

Electrolyte concn. mM	Dielectric parameters observed					Phase parameters calculated								
						by general formulas ^{a)}						by approximate formulas ^{b)}		
	C_I pF	C_h pF	G_I μ S	G_h μ S	f_0 kHz	C_I C_h	C_a pF	C_b pF	G_a μ S	G_b μ S	f_0 kHz	$10^4 \kappa_a^{c)}$ κ_b	C_a pF	G_a μ S
In distilled water														
0.0	1285	22.4	0.66	2.15	0.18	57.4	2632	22.6	0.945	2.19	0.188	1.25	2676	0.952
In NaOH aqueous solution														
0.06	700	22.5	14.2	27.5	3.0	31.1	2872	22.7	28.9	27.9	3.13	2.99	2993	29.4
0.125	790	22.5	28.2	59.5	6.5	35.1	2756	22.7	52.8	60.5	6.49	2.53	2855	53.6
0.25	865	22.5	54.8	121.7	12	38.4	2774	22.7	98.4	123.7	12.7	2.30	2862	99.7
0.5	950	22.5	102	246	25	42.2	2698	22.7	172.2	250	24.7	1.99	2772	174.3
1.0	1040	22.5	195	516	50	46.2	2625	22.7	310	525	50.2	1.71	2687	313
In KOH aqueous solution														
0.03	1121	22.9	6.19	17.85	1.6	49.0	2572	23.1	9.39	18.17	1.69	1.52	2627	9.48
0.06	894	23.0	15.6	37.9	4.0	38.9	2507	23.2	26.2	38.6	4.07	2.01	2583	26.5
0.125	1057	23.1	42.8	115.2	12	45.8	2614	23.3	67.4	117.3	11.2	1.71	2676	68.1
0.25	1164	24.0	78.6	230	21	48.5	2634	24.2	118.4	234	21.1	1.56	2690	119.5
In polystyrene sulfonate aqueous solution														
0 d)	633	22.1	0.779	1.56	0.20	28.6	2416	22.3	1.53	1.59	0.203	2.74	2526	1.56
0.05	610	23.7	2.04	3.90	0.50	25.7	2559	22.3	4.20	3.97	0.504	3.01	2682	4.28
0.1	710	24.2	3.24	6.78	0.80	29.3	2506	22.3	6.11	6.90	0.819	2.52	2604	6.21
0.2	833	24.4	4.62	10.9	1.2	34.1	2433	22.3	7.91	11.10	1.23	2.03	2509	8.02
0.4	860	24.4	7.83	18.8	2.0	35.2	2452	22.3	13.25	19.14	2.08	1.97	2526	13.4
0.8	1080	24.4	12.8	35.8	3.5	44.3	2560	22.4	19.73	36.4	3.46	1.55	2617	19.9
2.0	1280	24.5	23.5	80.2	7.0	52.2	2520	22.4	33.0	81.6	7.17	1.16	2561	33.2

Film thickness, $t=4.23 \mu\text{m}$; Film area, $S=4.68 \text{ cm}^2$ (diameter= 2.44 cm); Disc electrode diameter= 2.0 cm .

a) Calculated from the observed C_I , C_h , G_I and G_h by use of the general formulas Eqs. 26 to 40.

b) Calculated from the observed C_I , C_h , G_I and G_h by use of the approximate formulas Eqs. 56 and 58.

c) Calculated from G_a , G_b , C_b , ϵ_b , S and t by use of Eqs. 62 and 63.

d) Concentration in 0.01% units (W/V).

Table III. Dielectric Parameters Observed and Phase Parameters Calculated for the Cell Systems with
a Polystyrene Film and the Ambient Electrolyte Solution at 20°C

Electrolyte concn. mM	Dielectric parameters observed					Phase parameters calculated by general formulas ^{a)}						$\frac{10^5 \kappa_a^{b)}$ κ_b
	$\frac{C_l}{\text{pF}}$	$\frac{C_h}{\text{pF}}$	$\frac{G_l}{\mu\text{S}}$	$\frac{G_h}{\mu\text{S}}$	$\frac{f_0}{\text{kHz}}$	$\frac{C_l}{C_h}$	$\frac{C_a}{\text{pF}}$	$\frac{C_b}{\text{pF}}$	$\frac{G_a}{\mu\text{S}}$	$\frac{G_b}{\mu\text{S}}$	$\frac{f_0}{\text{kHz}}$	
In KCl aqueous solution												
0.03	1003	23.4	2.03	16.3	2.4	42.9	1295	23.8	2.31	16.9	2.32	8.54
0.06	1044	23.4	3.42	32.3	5.0	44.6	1295	23.8	3.81	33.5	4.50	7.11
0.125	1043	23.4	6.02	62.5	9.0	44.6	1267	23.8	6.64	64.9	8.82	6.40
0.25	1100	23.4	8.86	113.4	16	47.0	1286	23.8	9.58	117.6	15.5	5.09
In Bu ₄ NCl aqueous solution												
0.06	1133	23.4	1.07	17.7	2.5	48.4	1277	23.8	1.14	18.5	2.40	3.85
0.125	1140	23.4	1.70	32.2	4.5	48.7	1265	23.8	1.79	33.4	4.35	3.35
0.25	1157	23.4	3.33	65.2	9.0	49.7	1280	23.8	3.50	67.7	8.67	3.24
In Am ₄ NCl aqueous solution												
0.03	1157	23.4	0.643	11.6	1.6	49.7	1291	23.8	0.679	12.0	1.54	3.53
0.06	1158	23.4	0.941	19.3	2.5	49.5	1275	23.8	0.987	20.0	2.57	3.09
0.125	1150	23.4	1.58	34.0	4.5	49.1	1260	23.8	1.654	35.3	4.57	2.94
0.25	1158	23.4	3.16	65.6	9.0	49.5	1273	23.8	3.31	68.1	8.76	3.05

Film thickness, $t=8.70 \mu m$; Film area, $S=4.68 cm^2$ (diameter=2.44 cm).

Relative permittivity of water, $\epsilon_b=80$.

a) Calculated from the observed C_l , C_h , G_l and G_h by use of the general formulas Eqs. 26 to 40.

b) Calculated from the G_a , G_b , C_b , ϵ_b , S and t by use of Eqs. 62 and 63.

at frequencies higher than 100 kHz. Hence the conductance and capacitance values at lower frequency side of this minute relaxation were adopted as G_b and C_b in Table II. In this instance, care has to be taken on the evaluation of κ_b by use of Eq. 63, since effective values of ϵ_b for the polystyrene sulfonate solution must be different from that of distilled water. Hence, the ratio l/A was first calculated from Eq. 63 by use of the values of ϵ_b and C_b for distilled water. Next, values of κ_b for polystyrene sulfonate solutions were calculated from Eq. 63 by use of the value of l/A obtained above and the value of G_b evaluated for the film system with a polystyrene sulfonate solution.

Some distinctive features of this polystyrene film are found in the results summarized in Table II. The film capacitance C_a remained unchanged irrespective of electrolyte species and concentrations, giving a mean value $C_a(\text{mean})=2595$ pF. With this value, relative permittivity ϵ_a of the film was calculated from Eq. 61 to be 2.65, which is in good agreement with the previous estimation¹⁾.

The film conductance G_a was not inherent in the film itself but varied in proportion to the conductance G_b of the aqueous solution. In other words, the conductivity ratio κ_a/κ_b of the film to the solution must be almost unchanged with the electrolyte concentration in the solutions. This was roughly confirmed with the values of κ_a/κ_b calculated from Eqs. 62 and 63 as shown in Table II.

The present polystyrene film is the same as used in the previous experiments shown in Table 1 in reference 1. It can be concluded, therefore, that the present electrolytes NaOH, KOH and polystyrene sulfonate show somewhat high values of κ_a/κ_b as compared with some electrolytes such as KCl, HCl and CaCl_2 , which showed the values of κ_a/κ_b in a range $(5-8) \times 10^{-5}$.

The features of films capacitance C_a and conductivity ratio κ_a/κ_b independent of the electrolyte species and concentrations suggest that micropores in the films filled with the ambient electrolyte solutions are responsible for the electric conduction of the present underwater film.

4.3 Effect of Molecular Size on the Film Conduction

In a similar manner, dielectric analysis was carried out for the cases with solutions of KCl, tetrabutylammonium chloride (Bu_4NCl) and tetraamylammonium chloride (Am_4NCl), the results being summarized in Table III.

The features for C_a and κ_a/κ_b as seen in Table II are found also in Table III. The film capacitance C_a remained unchanged irrespective of electrolyte species and concentrations. The data of film capacitance shown in Table III gave a mean value $C_a(\text{mean})=1278$ pF, with which the relative permittivity ϵ_a was calculated to be 2.68.

The values of G_a are in proportion to those of G_b , giving the ratios κ_a/κ_b insensitive to the electrolyte concentrations. The average of the conductivity ratios κ_a/κ_b is 6.78, 3.48 and 3.15 in 10^{-5} units for KCl, Bu_4NCl and Am_4NCl respectively. This sequence of numerical values is in accordance with a reverse order of molecular sizes, suggesting the migrating ability of the ions across the underwater film.

V. CONCLUSIONS

1. General formulas were derived to calculate the phase parameters C_a , C_b , G_a and G_b

from dielectric parameters C_l , C_h , G_l and G_h characterizing the dielectric relaxations due to interfacial polarization for the bilamellar structure.

2. Approximate formulas for the C_l , C_h , G_l and G_h were derived from the general formulas under the condition $C_l/C_h \gg 1$.

3. Examination in the application of the theoretical formulas to dielectric observations for the lumped impedance models showed that the general formulas gave the phase parameters C_a , C_b , G_a and G_b within errors less than 1.5% for any case, whereas the approximate formulas can be used in practice within errors of 1% for the cases with $C_l/C_h \gtrsim 70$.

4. The theoretical formulas were also applied to the dielectric observations on systems of underwater polystyrene films to obtain the film capacitance and conductance. The general formulas applied to the observations gave the film capacitance which is unaffected by the electrolyte species and concentrations of the ambient solutions, giving the film relative permittivity of 2.65.

ACKNOWLEDGMENTS

The authors are grateful to Mr. K. Fujino of Mitsubishi-Monsanto Chemical Co. for kindly supplying the polystyrene specimens. Thanks are also due to Professor T. Kondo and Dr. M. Arakawa of Science University of Tokyo for kindly supplying a polystyrene sulfonate specimen.

REFERENCES

- (1) H. Z. Zhang, K. Sekine, T. Hanai and N. Koizumi, *Membrane*, **8**(4), 249 (1983).
- (2) T. Hanai, Electrical Properties of Emulsions, in "Emulsion Science," Chapter 5, edited by P. Sherman, Academic Press, London and New York, 1968, pp. 353-478.
- (3) S. B. Sachs, A. Raziell, H. Eisenberg and A. Katchalsky, *Trans. Faraday Soc.*, **65**, 77 (1969).
- (4) A. Minakata, *Biopolymers*, **11**, 1567 (1972).
- (5) F. van der Touw and M. Mandel, *Biophys. Chem.*, **2**, 231 (1974).
- (6) M. Mandel and F. van der Touw, Dielectric Properties of Polyelectrolytes in Solution, in "Charged and Reactive Polymers, vol. 1, Polyelectrolytes," ed. by E. Sélégny, D. Reidel Pubs. Co., Dordrecht-Holland, 1974, pp. 285-300.